



USER'S MANUAL: FIELD CAMERA UNIT INSTRUMENT HANDBOOK

WSO-FCU-SOC-MA-0001 Issue "Draft"

Approved by

Date

Signature

UCM

Ana Inés Gómez de Castro

INASAN

Mikhail Sachkov

Agreed by

Date

Signature

LA

Approval:

Issue		
Draft 0.0		
Author(s)	Date	
Ana I Gómez de Castro Andrey Shugarov Juan Carlos Vallejo	September 30 th , 2018	
Revised by	Date	
Ana Inés Gómez de Castro		
Approved by	Date	
Ana Inés Gómez de Castro		
Mikhail Sachkov		
Agreed by	Date	

Change Log:

Version	Date	Pages	Changes
Draft	30-Sept-18	25	First version
Revised version	07-Feb-19	25	Revised version including filters and detector gain update
Revised version	19-May-21	25	Revised version including few new details on the architecture of the detector

Table of Contents

1. Introduction.....	5
1.1 Purpose	5
1.2 Scope	5
1.3 Definitions and acronyms.....	6
1.3.1 Definitions	6
1.3.2 Acronyms.....	7
2 References.....	8
2.1 Reference Documents	8
3 The Field Camera Unit in WSO-UV.....	9
3.1 WSO-UV Science Instruments	9
4 FCU design, capabilities and operation modes	10
4.1 Optical design	11
4.1.1 Calibration Lamp Systems:	11
4.2 Detectors	12
4.3 FCU Operational Modes	12
4.4 Performance	12
5 Detectors Performance	14
5.1 The CCD Detector.....	14
5.1.1 CCD Photometric Response - Flat Fields.....	16
5.1.2 CCD Shutter Effects on Exposure Times	16
5.1.3 Read noise, charge transfer efficiency and dark current.....	16
5.2 The MCP detector	17
5.2.1 Bright objects limit.....	19
5.2.2 MCP Operation Modes	19
6 Imaging.....	20
6.1 FCU performance simulator	21
7 Prism/Grism Spectroscopy	22
7.1 P122 prism.....	23
7.2 P155 prism.....	23
8 Observation planning.....	23

Figure 3.1: Focal plane layout. Entrance slits to WUVS and fine guiding sensors are marked. The location of FCU pick-off mirrors is also indicated.	10
Figure 4.1: FCU channels location on the optical bench. In the UVO channel, the beam is directly sent from the on-axis pick-off mirror to the CCD detector in the UVO channel. In the FUV channel, two extra mirrors are added to correct from off-axis astigmatism, improve image quality and enlarge de focal ratio (see Fig. 4.2).	11
Figure 4.2: FCU/FUV optical design.	11
Figure 4.3: Throughput of the FCU (only mirrors and detectors are considered for the plot).	12
Figure 5.1: CCD 272 architecture.	14
Figure 5.2: Variable thickness of CCD AR coating.	15
Figure 5.3: Optimizations of CCD readout and AR coating	16
Figure 5.4: Foreseen quantum efficiency of FCU CCD in the UV range (with quantum yield effect).	16
Figure 5.5: Sketch of the vacuum sealed MCP detector.	17
Figure 5.6: MCP detector gain propagation.	18
Figure 5.7 One-axis projection PSF of the output photons shower from the P46 as sampled by the 10 μm diameter fibers; dotted lines mark the centre of the bins. This PSF is detected by the CMOS and the centroid is computed. This centroid determines the location of the photon impact on the photocathode surface.	19
Figure 5.8 Representation of the optical fibers bundle on the CMOS pixeled surface. On the left panel, the microtubes arrangement is outlined; each microtube has a projected section of 12 μm because of the pitch. In the central panel, the CMOS read-out is shown; each CMOS pixel has a size of 5.5 μm^2 . In the right panel, the MCP microtubes are projected on the CMOS surface; the projected diameter of the microtubes is 3.4 μm	19
Figure 6.1: Transmission curves for the FUV channel filters.	20
Figure 6.2: Transmission curves for the UVO channel broad band filters.	21
Figure 6.3: Transmission curves for the UVO channel narrow band filters.	21
Figure 6.4: Output from the WSOUV/FCU simulator of the performance of the FUV channel. The size of the field is 150x150 pix^2 . No filter is used in this simulation.	22
Figure 6.5: Output from the WSOUV/FCU simulator of the performance of the UVO channel. The size of the field is 400x400 pix^2 . No filter is used in this simulation.	22
Figure 7.1: Dispersion curve for the prisms in the FCU/FUV channel.	23

1. Introduction

1.1 Purpose

This document includes a first appraisal of Field Camera Unit (FCU) performance and operational modes to be released together with the WSO-UV call for Core Program Proposals requiring preparatory activities. The document describes the main optical elements, performance and operational modes of the FCU, in support to applicants for the call.

1.2 Scope

This document is produced on the frame of the development of the WSO-UV Ground Segment, as part of the Spanish Contribution to the WSO-UV mission, under contract of the Ministerio de Economía y Competitividad (MINECO).

1.3 Definitions and acronyms

1.3.1 Definitions

Table 2.1: Definitions

Concept	Definition

1.3.2 Acronyms

Table 2.2: Acronyms

Acronym	Definition
ACS	Advanced Camera System
AR	Anti Reflection coating
CCD	Charge Coupled Device
CMOS	Complementary Metal Oxide Semiconductor
CSV	Character Separated Values (data format)
ETC	Exposure Time Calculator
FCU	Field Camera Unit
FGS	Fine Guidance System
FUV	Far Ultraviolet
JCUVA	Joint Center for UltraViolet Astronomy
LSS	Long Slit Spectrograph
MCP	Micro Channels Plate
MINECO	Ministerio de Economía y Competitividad
NUV	Near Ultraviolet
PDR	Preliminary Design Review
PSF	Point Spread Function
QE	Quantum Efficiency
ROI	Region Of Interest
SDO	Solar Dynamics Observatory
SNR	Signal to Noise Ratio
TBC	To Be Confirmed
TBD	To Be Defined
UV	Ultraviolet
UVES	Ultraviolet Echellé Spectrograph
UVO	Ultraviolet-Optical
VUVES	Far Ultraviolet Echellé Spectrograph
WSO-UV	World Space Observatory-UltraViolet
WUVS	WSO-UV Spectrographs

2 References

2.1 Reference Documents

Table 2.1: Reference Documents

Ref.	Title	Code	Version/Date
[RD.01]	WSO-UV User's Handbook	WSO-USG-SOC-MA-0001	Issue 2.0 31-May-2018
[RD.02]	WSO-UV Science Policy – Core Programme	WSO-USG-SOC-LT-0001	Issue 1.0 31-May-2018
[RD.03]	WSO-UV Remote Proposal System Manual	WSO-GS-SOC-MA-0002	Issue 1.0 30-September-2018
[RD.04]	Manual to the Exposure Time Calculator for the FCU Instrument	WSO-GS-SOC-MA-0001	Issue 1.0 30-September-2018
[RD.05]	WSO-UV FCU Simulator User's Manual	WSO-GS-SOC-MA-0003	Issue 1.0 30-September-2018
[RD.06]	Manual to the Field Camera Unit Simulator	WSO-FCU-SOC-MA-0002	Issue 1.0 30-September-2018
[RD.07]	C. Jordi et al., Gaia broad band photometry, A&A 523, A48 (2010) DOI: 10.1051/0004-6361/201015441		
[RD.08]	Heyer, Biretta, et al. 2004, WFPC2 Instrument Handbook, Version 9.0 (Baltimore: STScI).		
[RD.09]	Dressel, L., 2019 “Wide Field Camera 3 Instrument Handbook, Version 11.0” (Baltimore: STScI)		
[RD.10]	http://galexgi.gsfc.nasa.gov/docs/galex/Documents/PostLaunchResponseCurveData.html		

3 The Field Camera Unit in WSO-UV

The Field Camera Unit (FCU) is the imaging instrument on board WSO-UV. The FCU has two independent channels that provide wide-field imaging in the near UV and optical range and high resolution far UV imaging capabilities respectively, using a set of filters to address a broad range of scientific goals. In addition, moderate capabilities for slitless spectroscopy are available in the far UV range. A third channel with coronagraphic capabilities is currently under consideration but decision on its final implementation is to be made in late 2019.

The FCU Instrument Handbook describes the instrument characteristics, expected performance, and operation modes and it is maintained by the FCU team at JCUVA. This first document is produced for the special core program call released in October 8th, 2018 for core program proposals that will require preparatory activities prior to November 2020 when the general call for core program proposals will be released. This is the basic technical reference manual to be used together with call specific documents and the Exposure Time Calculator, as reference for proposal writing; these documents are listed in Table 2.1 and can be downloaded from the WSO-UV JCUVA site.

This document is written in support to the first call for proposals for the WSO-UV core program. This first call is **only** for projects requiring preparatory observations with other facilities. The call is issued 4 years prior to the launch of the observatory to enhance the scientific efficiency of WSO-UV. It will guarantee astronomers core program observing time while running, in advance, preparatory observations for target selection or characterization. At this time, WSO-UV is not fully built, tested or calibrated. Applicants should be aware of this fact.

3.1 WSO-UV Science Instruments

The WSO-UV telescope feeds two main instruments: the spectrographs unit (WUVS) and field camera unit (FCU), as well as the Fine Guidance System (FGS). WSO-UV instrumentation is designed to provide:

- Spectroscopic observations in the 115-315 nm range with dispersion 50,000.
- Long slit spectroscopy with spectral dispersion 1,000.
- Imagery of space objects with high resolution (up to 0.1 arcseconds in the 115-176 nm range) and wide field imaging in the 174-600 nm range.

The focal plane layout is shown in Figure 3.1. The Fine Guiding Sensors are located in a circle of radius 24.25 arcmin around the T-170M optical axis. WUVS entrance slits are intercalated between them, to guarantee accurate guiding during the foreseen long spectroscopic observations. The FCU picks off the beam from the telescope axis but requires an independent refocussing mechanism for high resolution imaging since the FGS focuses the telescope beam on the entrance slits of the spectrographs.

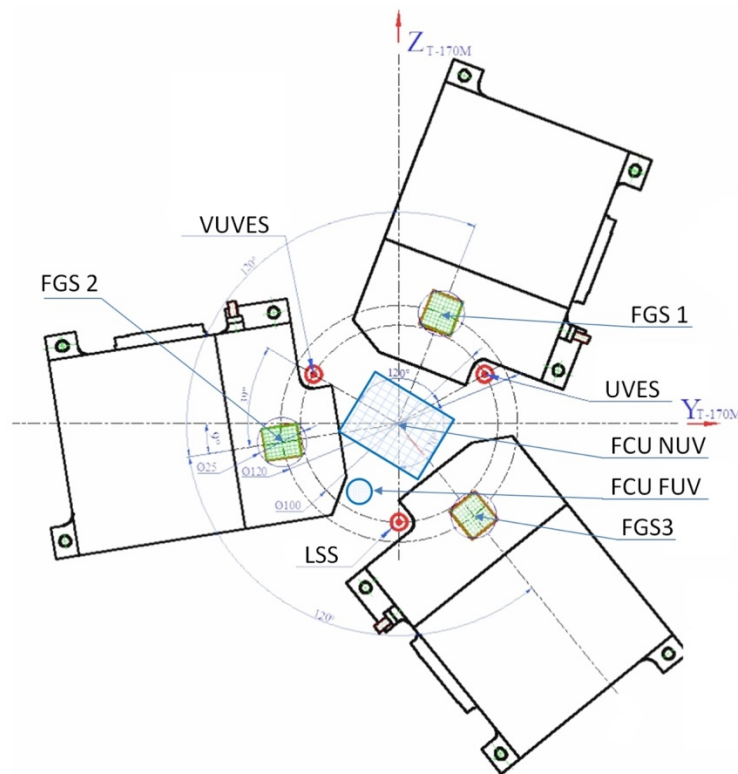


Figure 3.1: Focal plane layout. Entrance slits to WUVS and fine guiding sensors are marked. The location of FCU pick-off mirrors is also indicated.

4 FCU design, capabilities and operation modes

The FCU is mounted on top of the optical bench, below the primary mirror of the T-170M. The FCU has two channels, each fed by an independent pick off mirror. The far UV (FUV) channel has capabilities for high resolution imaging. Also, some low dispersion spectroscopic capabilities around Lyman-alpha (121.5 nm) and the C IV resonance transition at 155.0 nm are available. The UV-optical (UVO) channel is designed for wide field imaging from 174 to 600nm. The main features of the FCU are summarized in Table 4.1.

Table 4.1: Main features of the WSO-UV FCU.

Parameters	FUV channel	UVO channel
Detector	MCP	CCD
Spectral Range (nm)	115-176	174-600
Effective Area (m ²)	0.23 at 122 nm	1.1 @ 255 nm
Field of View	Ø 1.40 arcmin diameter	10x7.5 arcmin ²
Scale	0.041 arcsec/microchannel*	0.146 arcsec/pixel
Detector Format	2k x 2k	4k x 3k
Number of Filters	Up to 10 + 2prisms	Up to 15

*The section of the MCP micro-channels has a diameter of ~10 microns; given the channels pitch angle the projected detection element of 12 microns.

4.1 Optical design

The FCU layout is shown in Figure 4.1. Only a fraction of the optical bench is occupied and baffled from the rest; this extra space would be occupied by the third channel, if finally funded.

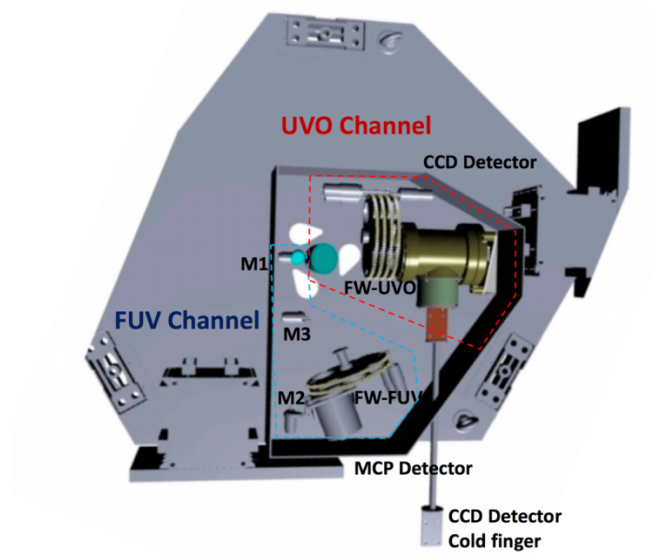


Figure 4.1: FCU channels location on the optical bench. In the UVO channel, the beam is directly sent from the on-axis pick-off mirror to the CCD detector in the UVO channel. In the FUV channel, two extra mirrors are added to correct from off-axis astigmatism, improve image quality and enlarge de focal ratio (see Fig. 4.2).

The optical design of the UVO channel is very simple; the beam is picked off directly from the telescope axis and focused on the CCD detector (F/10). There are four filter wheels in the light path, one of them to be used as a shutter. The FCU/FUV optical chain comprises three aluminized mirrors coated with MgF₂, shown schematically in Figure 4.2.

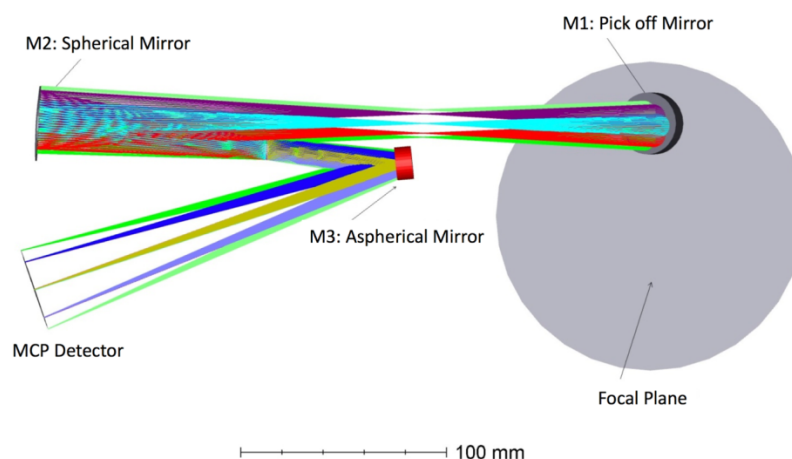


Figure 4.2: FCU/FUV optical design.

4.1.1 Calibration Lamp Systems:

FCU calibration lamp systems are under development.

4.2 Detectors

The FCU channels have the following detectors:

- The UVO channel uses a 4096 x 3112 Teledyne-e2V CCD with $12 \times 12 \mu\text{m}^2$ pixels and spatial resolution ~ 0.146 arcsec/pixel, resulting in a nominal 598×448 arcsec² field of view (FOV). The spectral sensitivity ranges from ~ 174 nm to ~ 600 nm, with a peak efficiency of 48% at ~ 230 nm.
- The FUV channel detector is a solar-blind CsI microchannels plate (MCP) with Complementary Metal Oxide Semiconductor (CMOS) detector readout. The CMOS is a 2048×2048 pixels array, each pixel of $5.5 \times 5.5 \mu\text{m}^2$ in size. The scale on the detector is 0.04 arcsec per microchannel producing a nominal FoV of 1.4×1.4 arcmin². The spectral response ranges from ~ 115 nm to ~ 176 nm with a peak efficiency of 20% at 125 nm.

4.3 FCU Operational Modes

FCU will support imaging modes in both FUV and UVO channels. Moreover FCU/UVO would be used in parallel mode during spectroscopic observations. The supported modes are:

- **Imaging:** The beam is focused on the selected channel (FUV or UVO).
- **Imaging Time-tag:** Photon counting image mode on 80×80 pixels on the detector. Photons will be count at a pace of at most 40 ms/read-out over 5 minutes. This mode is *only available in the FUV channel*. It may require a previous acquisition image to set the target in a pre-defined area of fast read-out.
- **Spectroscopy:** The beam is directed to the prisms. It may require refocusing the camera. This mode is *only available in the FUV channel*.
- **Spectroscopy Time-Tag:** Photon counting slitless spectroscopy mode on 20×300 pixels on the detector. Photons will be count at a pace of at most 40 ms/read-out over 5 minutes. This mode is *only available in the FUV channel*. It may require a previous acquisition image to set the target in a pre-defined area of fast read-out.
- **Parallel-UVO:** FCU/UVO Channel is used in parallel mode while using any other instrument.

4.4 Performance

The throughput of the FCU is shown in Figure 4.3 and the preliminary filter list in Table 4.2. FCU PDR will be at the end of 2018. There may be slight changes in the quoted performances.

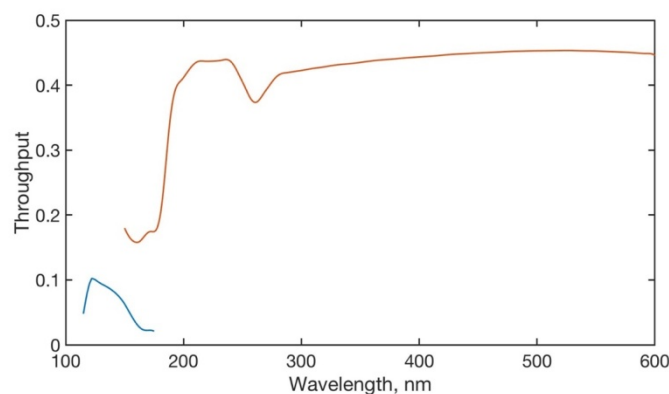


Figure 4.3: Throughput of the FCU (only mirrors and detectors are considered for the plot).

Table 4.2: Filters and dispersive elements in the WSO-UV/FCU (transmission curves available online).

FILTER NAME	DESCRIPTION
FILTERS FOR THE FCU/FUV CHANNEL	
F125LP	Step filter: Transmittance 0 for wavelengths below 1250Å and Transmittance 1 for wavelengths above 1250Å
F140LP	Step filter: Transmittance 0 for wavelengths below 1400Å and Transmittance 1 for wavelengths above 1400Å
F150LP	Step filter: Transmittance 0 for wavelengths below 1500Å and Transmittance 1 for wavelengths above 1500Å
F165LP	Step filter: Transmittance 0 for wavelengths below 1650Å and Transmittance 1 for wavelengths above 1650Å
G010	Grey filter that blocks 90% of the radiation to observe bright fields.
DISPERSIVE ELEMENTS FOR THE FCU/FUV CHANNEL	
P122	Prism with peak dispersion $D=600$ at 1215 Å , decreasing to $D=200$ at 1400 Å
P155	Prism with peak dispersion $D=1400$ at 1400 Å , decreasing to $D=600$ at 1550 Å
FILTERS FOR THE FCU/UVO CHANNEL	
G _{BP}	GAIA BP filter [RD.07]
F185W	[RD.08]
F255W	As F255W [RD.08]
F336W	As F336W [RD.08]
F555W	V-band [RD.08]
F232N	A 50Å passband (FWHM) Gaussian filter centred at $\lambda_2 323\text{Å}$ with maximum transmittance at this wavelength
F280N	A 50Å passband (FWHM) Gaussian filter centred at $\lambda_2 800\text{Å}$ with maximum transmittance at this wavelength
F308N	A 50Å passband (FWHM) Gaussian filter centred at $\lambda_3 080\text{Å}$ with maximum transmittance at this wavelength
F656N	A 50Å passband (FWHM) Gaussian filter centred at $\lambda_6 563\text{Å}$ with maximum transmittance at this wavelength
F673N	A 100Å passband (FWHM) Gaussian filter centred at $\lambda_6 730\text{Å}$ with maximum transmittance at this wavelength
F250LP	A red-leak filter with transmittance 0 for wavelengths above 2500Å .
F438W	B-band [RD.09]
F606W	Wide V [RD.09]
F814W	I-band [RD.09]
GLnuv	GALEX NUV Band filter [RD.10]

5 Detectors Performance

FCU employs two fundamentally different types of detectors: a CCD from the near-UV to the Visible (UVO Channel), and a Micro Channels Plate (MCP) detector for use in the far-UV (FUV Channel). The CCD and the MCP detectors impose limitations on the feasibility of observations. This describe the detectors essentials to ensure the feasibility of observations.

5.1 The CCD Detector

CCDs for WSO-UV have been manufactured by Teledyne-e2v, a company with a long heritage in manufacture of UV sensitive image devices (CCDs and CMOS), mainly for solar observation missions including Stereo (SECCHI), Solar Dynamic Observatory, SXI. WSO-UV detector is a modified version of the device used for ESA's EUCLID mission.

The basic device layout is shown schematically on Fig. 5.1. The pixel size of CCD272 is 12 μm square but pixels can be combined in 2×2 groups to give an effective 24 μm pixel. The CCD utilises differential outputs to enable common mode noise suppression. FCU CCD detector is optimized to operate at low level signals.

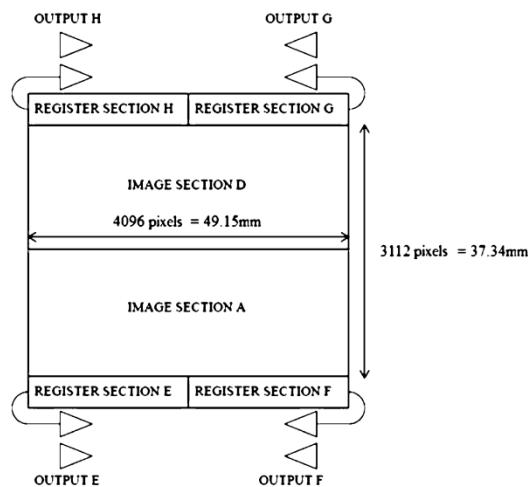


Figure 5.1: CCD 272 architecture.

The detector system consists of three main components:

- a UV sensitive CCD;
- a hermetically sealed vacuum enclosure with a UV transmission window;
- flight electronics and cabling based on existing heritage but with a new detection chain with digital correlated double sampling.

A mechanical shutter is located in the light path to block the light during CCD readout procedure. Detectors will operate at the temperature of 173 K with 600 s standard integration time. CCD detectors are optimised for low read-out noise (less than 3 e⁻) and low dark current (Table 5.1).

Key features that make the device suitable for FCU are:

- UV Enhanced Process.
- Anti-reflection coating of parts of the devices.
- Low clock voltages.
- Split frame transfer.
- Two phase image area for best charge transfer.

Radiation in the range of 100 nm to 300 nm is the most difficult to be detected with silicon. This is because the absorption depth is small at these wavelengths. This means that the CCD must be thinned to minimize any dead layer at the back surface. To optimize the QE the anti-reflection coating of different thickness is used (Figs. 5.2 and 5.3). CCD chips with no anti-reflection (AR) coating for FUV range (<200 nm) and AR coating for NUV range (>200 nm) have been manufactured by the enhanced back-thinned process.

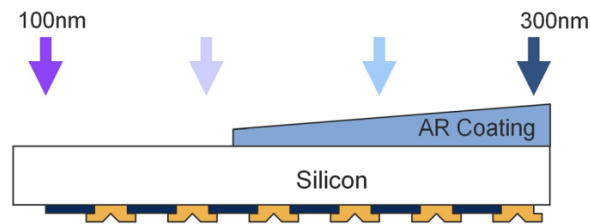


Figure 5.2: Variable thickness of CCD AR coating.

Split frame transfer CCD architecture with two phase image section design is used to provide maximum charge transfer efficiency after radiation. The CCD uses a low voltage process to minimize power consumption both on the device and in the drive electronics.

Table 5.1: Main characteristics of the CCD detector.

Main characteristics	
Spectral range, nm	174-600
Size of photosensitive area, mm	37.3x49.1
Pixel size, μm	12
Readout speed, kHz	50, 100, 500
Readout noise at 50 kHz, not more than, e ⁻ , sd	3
Readout noise at 100 kHz, not more than, e ⁻ , sd	3.5
Readout noise at 500 kHz, not more than, e ⁻ , sd	7
Digitalization	14 bits
Full well capacity, e ⁻	30000
Dark current, not more than, e ⁻ /pixel/hour:	
at the beginning of life	12
at the end of life	36
Exposure time, sec	1-3600
Dynamic range in one frame	10000:1

For a number of Teledyne-e2v CCDs supplied to the SXI, Stereo-SECCHI and SDO the quantum efficiency in UV was measured. Excellent QE stability against illumination overload was shown. The predicted

quantum efficiency of the CCD and detector system is shown on Fig. 5.4. The CCD spectral range for uncoated region will be 115-1000 nm.

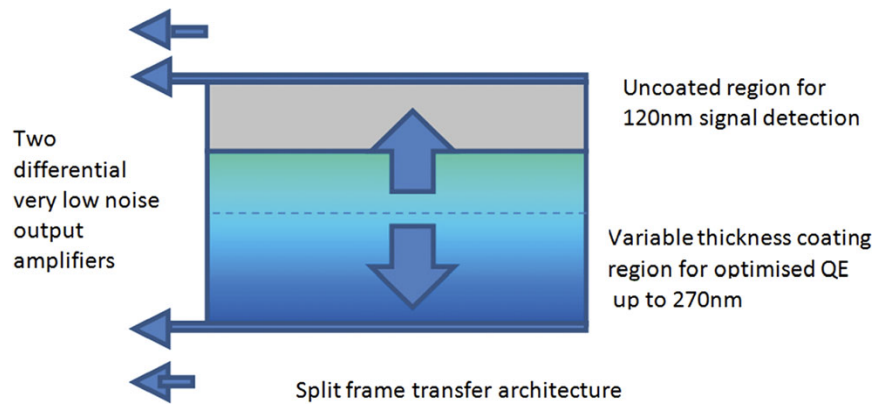


Figure 5.3: Optimizations of CCD readout and AR coating

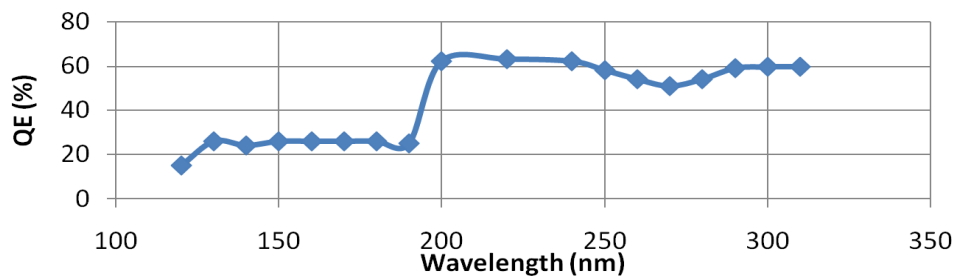


Figure 5.4: Foreseen quantum efficiency of FCU CCD in the UV range (with quantum yield effect).

5.1.1 CCD Photometric Response - Flat Fields

The CCD response will be measured in ground-based facilities and further tested on flight. The reference images for flat fielding will include:

- Ground-based flats with signal-to-noise ratios of ~300 per pixel for all filters.
- Flats to measure the pixel-to-pixel and intra-pixel variations that will be obtained from in-flight dithered observations of the same rich stellar fields used by the Hubble Space Telescope Instruments, in particular, by the Advanced Camera System (ACS) (see ACS ISRs 2002-08 and 2003-10).

5.1.2 CCD Shutter Effects on Exposure Times

The shutter in the UVO channel is designed to be very fast and will affect by less than 1% the photometry for the shortest possible exposure (1 s).

5.1.3 Read noise, charge transfer efficiency and dark current

The expected performance of the CCD in terms of read noise, charge transfer efficiency and dark current level is in Table 5.1. After the detector on-ground calibration further details on fringing, hot and bad pixels will be provided in this section. Further details on the fraction of pixels affected by cosmic rays during a long (~1000 second) exposure will be available at the end of the in-flight commissioning period.

5.2 The MCP detector

FCU MCP detector is a three steps detection system that transforms incoming UV photons into optical photons that are detected by a fast and configurable CMOS device (see Figure 5.5). The opaque CsI photocathode is deposited directly on the face of the MCP; the QE of CsI is very low ($\ll 0.1\%$) at wavelengths longer than 175 nm minimizing the contamination from Solar scattered light. Target photons strike the photocathode, liberating single photoelectrons which pass into the MCP, where a pulse of $\sim 1 \times 10^5 e^-$ is generated. In a second step, the electrons pulse is transformed into a photon pulse at the phosphor (P46) interface; the output photons showers are captured by a bundle of optical fibers that transport the signal to the CMOS detector. There is a fiber attached to each $5.5 \times 5.5 \mu m^2$ pixel on the CMOS. In the final step, the optical photons are detected by the CMOS. The main characteristics of the MCP detector are summarized in Table 5.2. The CMOS provider is AMS (CMOSIS) and the MCP provider is Photek. The detector design is based on the FUV detector implemented in the UltraViolet Imaging Telescope (UVIT) on Astrosat though performance in terms of sensitivity and read-out has been improved.

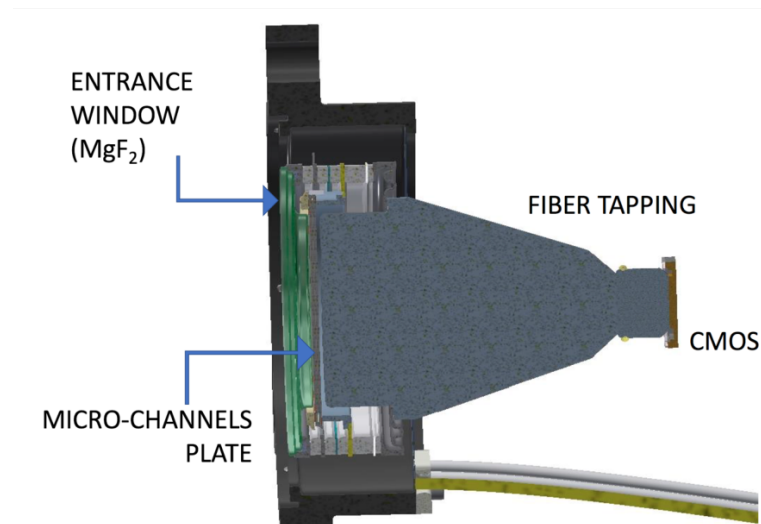
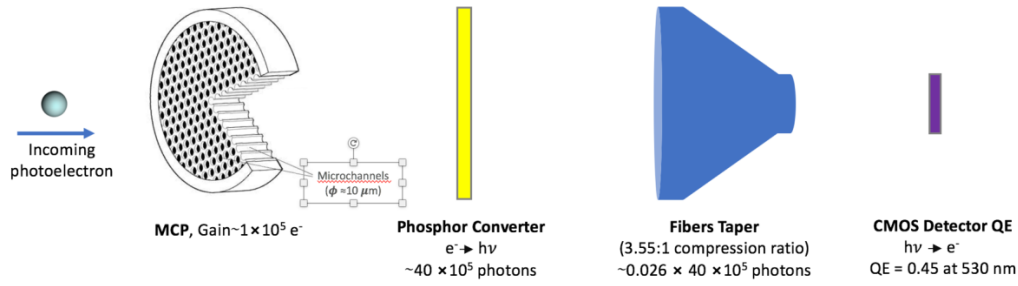


Figure 5.5: Sketch of the vacuum sealed MCP detector.

This complex detection system has been optimized to increase the gain and preserve the image optical quality at the entrance of the detector. The effect in gain is summarized in Figure 5.6; basically, a shower of 100,000 photons is generated at the MCP per UV photon at the entrance window. On board processing software is implemented to compute the centroid of the shower; for each event three parameters are determined: (x,y) coordinates on the entrance window and Δt , time lapse between the detection and the beginning of the exposure.



OUTCOME: 1 UV photon \Rightarrow 104,000 optical photons \Rightarrow 9,360 photoelectrons from the central pixel

Figure 5.6: MCP detector gain propagation.

Table 5.2: Main characteristics of the MCP detector

Main characteristics		
Spectral range, nm		115-176
Size of photosensitive area, mm		\varnothing 40
Pore diameter on MCP, μm		10
Pore pitch on MCP, μm		12
Optical taper compression factor	40 mm to 11.264 mm	3.55:1
Phosphor screen		P46
CMOS detector characteristics:	Size, pixels	2048x2048
	Pixel size, μm^2	5.5x5.5
	Readout speed, fps	
	Full frame (10bits):	180
	Full frame (12bits):	37
ROI windowing capability		Up to 8
Full well charge, e^-		13,500
Dark current, e^-/s (25°C)		125
Dynamic range, dB		60
INTEGRATED SYSTEM		
Dynamic range in one frame, dB		40
Maximum count rate, counts/s		TBD
Saturation count rate, counts/s	Full frame	200,000

At the Phosphor surface, the output photon shower has a typical FWHM of 60 micron¹ (see Figure 5.7). This is captured by the optical fibers of the fiber taper. The diameter of the fibers is 12 microns at the phosphor converter, at the other end, fibers are 3.3 micron, since the demagnification ratio is 3.62.

¹ These values are preliminary. The detector development team is trying to reduce the shower FWHM to 40 microns (or 11.3 microns on the CMOS surface).

Therefore, the shower is compressed into 16.2 micron on the detector² (or 3 pixels on the detector). The centroid of this shower is used to identify the microtube, on the MCP, where the UV photon has impacted.

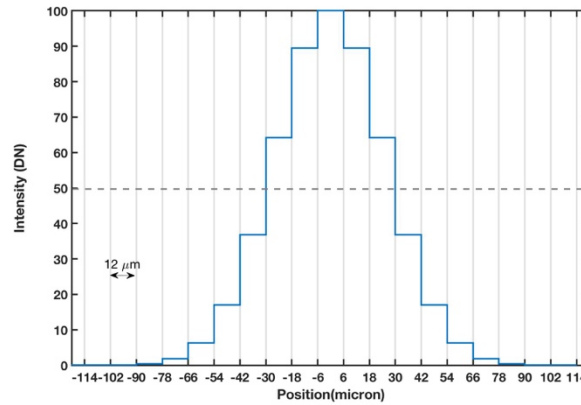


Figure 5.7 One-axis projection PSF of the output photons shower from the P46 as sampled by the 12 μm diameter fibers; dotted lines mark the centre of the bins. This PSF is detected by the CMOS and the centroid is computed. This centroid determines the location of the photon impact on the photocathode surface.

The section of the MCP is a hive of microtubes arranged in a hexagonal pattern. From end to end, the number of microtubes is $40 \text{ mm}/12 \mu\text{m} = 3,333$ micro tubes that project on the CMOS square grid made of 2048 pixels of 5.5 μm, as shown in Figure 5.7; 1.6 microtubes fit within a pixel in any given direction.

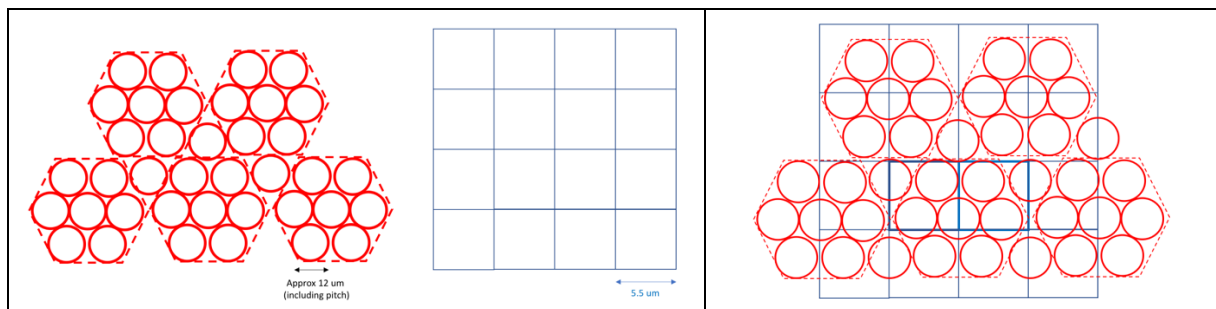


Figure 5.8 Representation of the optical fibers bundle on the CMOS pixelated surface. On the left panel, the microtubes arrangement is outlined; each microtube has a projected section of 12 μm because of the pitch. In the central panel, the CMOS read-out is shown; each CMOS pixel has a size of 5.5 μm². In the right panel, the MCP microtubes are projected on the CMOS surface; the projected diameter of the microtubes is 3.3 μm.

5.2.1 Bright objects limit

Over-extraction of charge from the microchannel plates causes permanent reduction of response and detector damage. To prevent it, safety limits will be defined both for local count rates and global count rates (see Table 5.2).

5.2.2 MCP Operation Modes

The MCP detector is a photon-counting device which processes events serially; it operates in four possible modes:

² Between the fiber taper and the CMOS there is an additional ND filter which has 4 micron fibers. This is coupled to the fiber block bonded to the CMOS which has fibers of diameter 3 microns.

- *Accumulation mode*: all counts received during the exposure at a given pixel on the CMOS are added together.
- *Time-tagged acquisition mode*: each event is time-tagged. This mode is available for a reduced area on the detector and with time resolution of 40 milliseconds.
- *High resolution mode*: refined centroiding algorithms are implemented to reach sub-pixel ($1/4^{\text{th}}$ to $1/8^{\text{th}}$ of a pixel) spatial resolution. This mode requires a nearby bright source in the field to correct for the spacecraft jittering and operates in a reduced area of the detector.
- *High gain mode*: to increase the SNR in low surface flux areas or during the observation of weak sources.

6 Imaging

FCU can be used to obtain images through a set of optical and ultraviolet filters. For the UVO channel three filters wheels, each with 6 slots are available. For the FUV channel two filters wheels, each with 6 slots is available. The desired filter in one filter wheel is rotated into position and a CLEAR aperture in the other filter wheel is automatically selected. In the FUV channel, there is an opaque filter in one of the slots so the wheel must only be rotated to block the beam if a bright object limit violation occurs.

The approved filters for imaging with each channel are summarized in Table 4.1; the list is not complete and further filters will be added to UVO channel. Figures 6.1 through 6.3 show the filter transmission curves. The full performance of the system can be computed using the WSO-UV FCU Exposure Time Calculator, available in the JCUVA, WSO-UV web site (see also ETC User's manual).

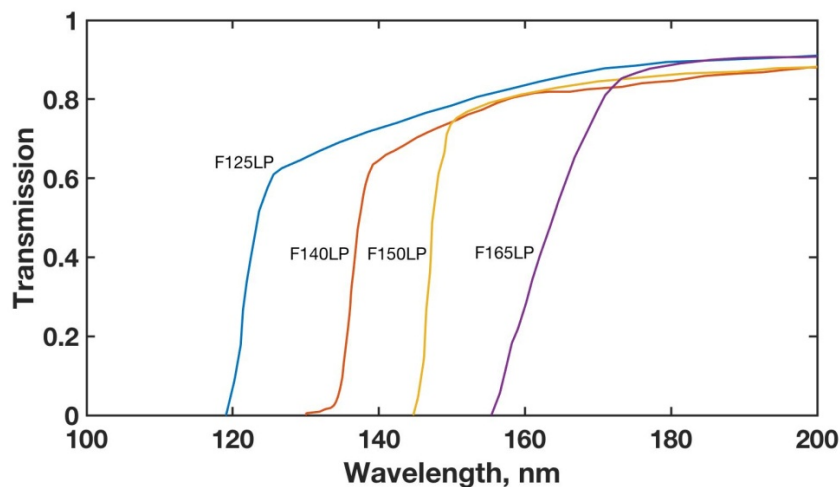


Figure 6.1: Transmission curves for the FUV channel filters.

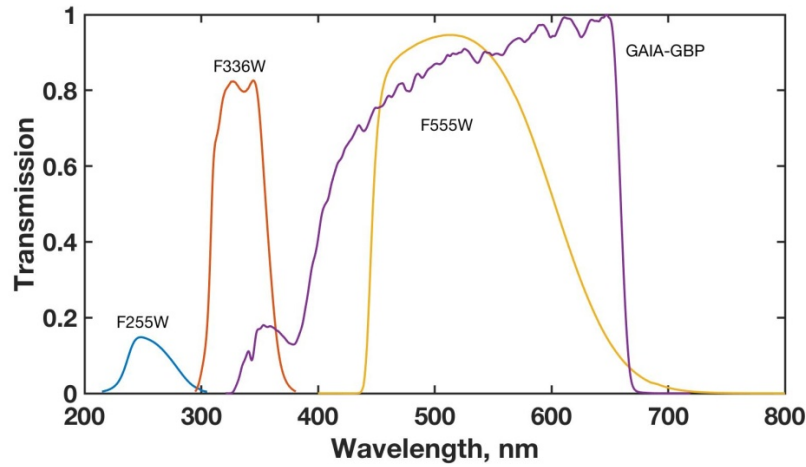


Figure 6.2: Transmission curves for the UVO channel broad band filters.

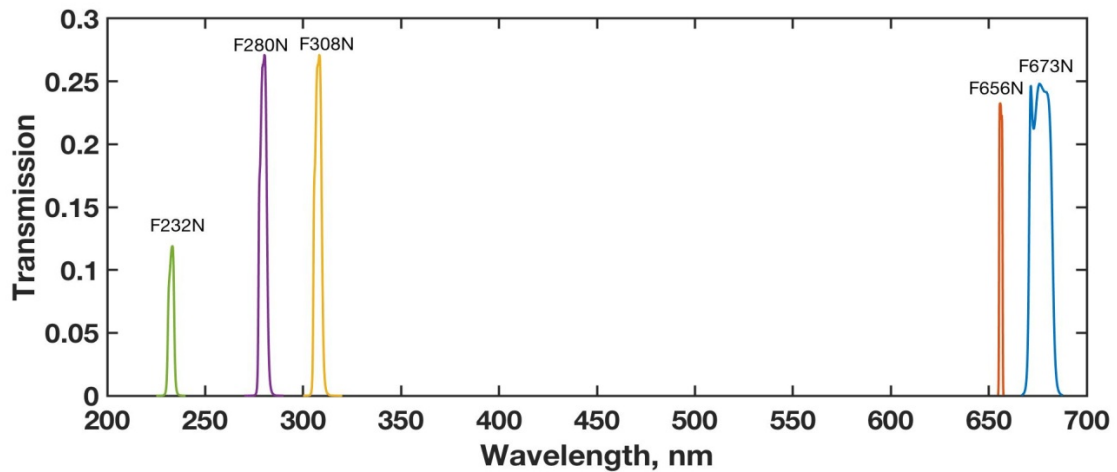


Figure 6.3: Transmission curves for the UVO channel narrow band filters.

6.1 FCU performance simulator

The WSO-UV team has made available to the community a computer tool, the FCU simulator that generates artificial images of stellar fields simulating the performance of the WSO-UV/FCU system. The software includes the optical system, the telescope jitter and the detector response. The coordinates of the point like sources to be simulated are to be provided in a CSV file together with their magnitudes in the relevant band. The tool is available in the JCUVA, WSO-UV web site (see also WSO-UV FCU simulator User's manual). In Figures 6.4 and 6.5, the output is displayed for a test field.

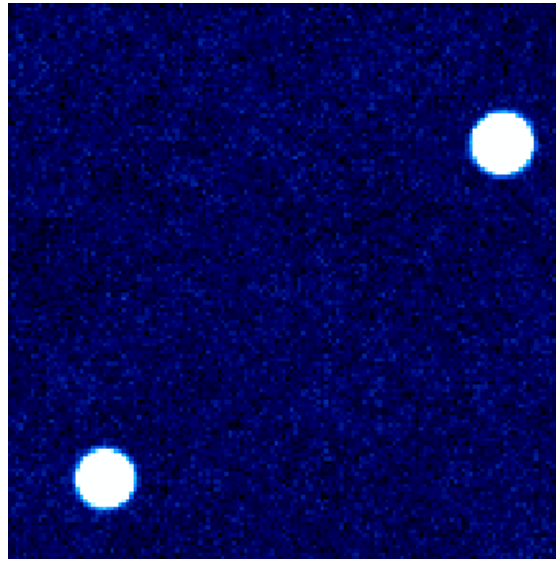


Figure 6.4: Output from the WSOUV/FCU simulator of the performance of the FUV channel. The size of the field is 150×150 pix². No filter is used in this simulation.

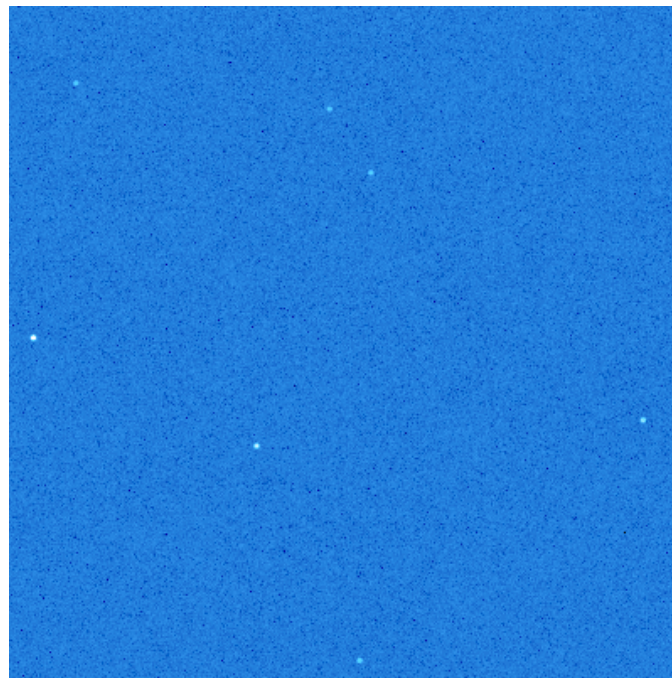


Figure 6.5: Output from the WSOUV/FCU simulator of the performance of the UVO channel. The size of the field is 400×400 pix². No filter is used in this simulation.

7 Prism/Grism Spectroscopy

One of the two filter wheels in the FUV channel includes two dispersing elements for low resolution slitless spectroscopy over the field of view: P122 and P155. Both elements are prisms hence providing

have non-linear dispersion with maximum resolution at shorter wavelengths and much lower resolving power at longer wavelengths (see Figure 7.1).

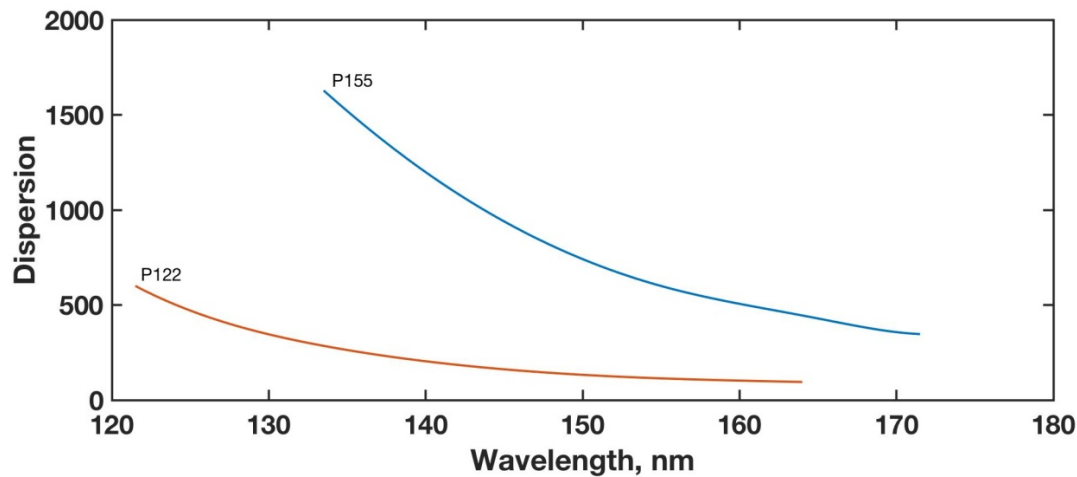


Figure 7.1: Dispersion curve for the prisms in the FCU/FUV channel.

7.1 P122 prism

P122 is designed to provide dispersions between 600 and 300 in spectral lines of astrobiological interest such as Lyman- α , O I ($\lambda = 130$ nm) or CII ($\lambda = 135$ nm) resonance transitions.

7.2 P155 prism

P155 is designed to provide dispersion 600 at the CIV resonance transition ($\lambda = 155$ nm) to enable measuring terminal velocities of the massive stars outflows in young star forming clusters in Local Group galaxies.

8 Observation planning

Observation planning for WSO-UV has been required to be very simple from the beginning of the project. Sequences of observations will be defined based on the approved scientific projects to later be optimized by the scheduler. The High Earth Orbit of WSO-UV guarantees a very efficient and versatile scheduling ideally suited for monitoring programs. Tools to assist applicants on the optimization of their proposals will be provided for the Phase II call.

At the time of planning observations with the WSO-UV/FCU, there are some few aspects you should carefully consider. These are:

- **Bright sources constraints.** Sources with photon counts above the FUV channel brightness limit must not be included in the list of observations. Note that the brightness limit depends on the variability of sources. Also note that though the CMOS detector has the capability of reading only ROIs, the full field of view illuminates the MCP that can be subsequently damaged by high count rates.
- Decide the observation mode for the FUV channel: **TIME TAG or ACCUM.** The TIME TAG mode is very versatile and allows photon counting to study the variability of all sources in the field of view; it is the most information efficient mode.
- Evaluate the implementation of **dithering** in your observations. Dithering will improve the spatial resolution and photometric quality of your images. This mode is highly recommended for imaging modes, especially for the wide field observation with the FCU/UVO channel. The

FCU/UVO PSF is undersampled by a factor ~ 2 at the optical limit (350 nm). It will be possible to achieve a final reconstructed FWHM of 0.146 arcseconds for well-dithered observations.

[End Of Document]